Hindawi
Shock and Vibration
Volume 2022, Article ID 9878557, 12 pages
https://doi.org/10.1155/2022/9878557

Research Article

Deformation Characteristics and Control Countermeasures for Surrounding Rock of Deep Roadway under Mining Disturbance: A Case Study

Deyu Qian,[1] **Jinping Deng**,[1] **Sujian Wang**,[2,3,4] **Xingguo Yang**,[1] **Qi Cui**,[1] **Zexiang Li**,[1] **Shengyao Jin**,[2] **and Wenjing Liu**[2]

[1]*School of Mines, China University of Mining and Technology, Xuzhou 221116, China*
[2]*Shaanxi Coal and Chemical Industry Technology Research Institute Co., Ltd, Shaanxi, Xi'an 710100, China*
[3]*The National Joint Engineering Research Center of the Green, Safe and Efficient Coal Mining, Xi'an 710065, China*
[4]*Sanqin Scholar Innovation Team, Shaanxi Coal and Chemical Industry Group Co, Ltd., Xi'an 710100, China*

Correspondence should be addressed to Deyu Qian; qian@cumt.edu.cn and Jinping Deng; dengjinping@cumt.edu.cn

Received 16 April 2021; Revised 10 August 2021; Accepted 11 March 2022; Published 5 May 2022

Academic Editor: Traian Mazilu

Highly efficient maintenance and control of the deep strong mining roadway's stability is a reliable guarantee for the safe production and sustainable development of a coal mine. With return air roadway 4106 in Wenjiapo coal mine as the research background, an in situ investigation, numerical simulation, and engineering practice were carried out to reveal the stress distribution and surrounding rock deformation and failure characteristics of a strong mining roadway. The numerical simulation results show that both first mining and secondary mining are positively correlated with the deformation and failure of roadway surrounding rock. The peak abutment pressure of the coal pillar near the goaf caused by first mining and secondary mining are 28.7 and 35.6 MPa, respectively, with a 24% increase. During the first mining period, the total deformation of the roof and floor of the roadway and the two sides was 1160 and 1436 mm, respectively. During the second mining period, the total deformation of the roof and floor of the roadway in a working face advance gradually increased from 1737 mm 80 m away from the working face to 2281 mm at the working face, and the total deformation of the two sidewalls gradually increased from 2094 mm 80 m away from the working face to 2211 mm at the working face. The damage to the roadway caused by secondary mining was much greater than that caused by the first mining. The collaborative control technology of long anchorage-top-cutting blasting stress relief is proposed to control the stability of the roadway. The engineering practice shows that the deformation of the roadway is effectively controlled under strong mining disturbance, and the maximum deformations of the roof, floor and sidewall are 17, 23, and 11 mm, respectively.

1. Introduction

With the development of deep coal mining, the roadway is faced with the multiple effects of "three highs and one disturbance." The deep rock mass shows obvious mechanical properties of soft rock such as nonlinear large deformation [1–5]. The disasters such as roof subsidence, floor heaving and water disaster bring great challenges to the stability control of the roadway surrounding rock [6–9]. In particular, the deformation and failure of the mining roadway under the effect of strong mining and low surrounding rock strength, a pair of "high stress-low strength" contradiction, is becoming more and more serious, and the difficulty of control increases sharply [10–13]. The newly excavated roadway in the Binhuang mining area of Shaanxi Province in China is growing by more than 50,000 meters per year. There are a large number of roadways with large deformation in this mining area. The roadways have long-term rheology under the action of a strong dynamic load and high stress superposition. The roof of the roadway is easy to break, the unevenness of the sidewall is bulging, and the floor heaving is intense. Controlling the rock surrounding the roadway has

become a technical problem that is restricting the production of the mine [14–17].

A large number of scholars have studied the problem of roadway surrounding rock control. Kang and Wang [18] proposed the theory of high prestressed and strong support according to the characteristics of a deep, high stress soft rock roadway and a large section open-off cut roadway. Huang et al. [19] studied the rheology of the surrounding rock floor and the large deformation theory of structural instability in a deep mining roadway and expounded the mechanism of floor heaving in a deep strong mining roadway. Zhang et al. [20] used a prestressed steel strand system to construct a thick and strong anchorage layer for a strong mining roadway in Sanhejian Coal Mine, combined with a high-performance prestressed bolt and short anchor cable, formed prestressed combined support technology, and achieved good results in a field engineering application. Li et al. [21] proposed "non-uniform support technology based on anchor grouting reinforcement and strengthened key parts," which solved the support problem of a strong mine pressure roadway. Yang et al. [22] studied the mechanical effect of a corner bolt in roadway surrounding rock control through numerical simulation and applied it to a mine successfully. However, due to the complex and changeable geological conditions, the understanding of the failure mechanism of roadway surrounding rock is not accurate enough. In actual engineering construction, the support scheme is mainly designed by engineering analogy methods and existing experience. It is difficult to meet the requirements of roadway support, and even excessive deformation leads to support failure, which seriously affects the safety production of the working face [23, 24].

Therefore, this study used FLAC^{3D} numerical calculation software to simulate and analyze the deformation and failure characteristics of return air roadway 4106 in Wenjiapo Mine under operation during first mining and secondary mining and analyzes the influence of two mining disturbances on the stability of the roadway. Based on the numerical simulation analysis, the surrounding rock control technology of the roadway is proposed. Finally, the field test of long anchorage-stress relief coordination control was carried out in the return air roadway 4106 in Wenjiapo Mine.

2. Engineering Background

The working face 4106 of Wenjiapo Mine is the sixth working face in goaf area 41. A 44.5-meter coal pillar is left between the return air roadway 4106 and the working face 4105 being mined. The working face is mainly mining coal seam #4, the length of the working face is 2010 m, the dip length is 218 m, with a mining height of 11 m, and all the roofs are treated using the collapse method. The roadway has a buried depth of 700~730 m, a width of 5500 mm, a height of 3850 mm, and a cross section of 19.4 m^2. The main roof is gray-white coarse-grained sandstone with an average thickness of 6.3 m; the immediate roof is gray-white medium-grained sandstone with an average thickness of 4.3 m; the immediate floor is dark gray mudstone with an average thickness of 1.7 m; the main floor is gray mudstone with an average thickness of 8.5 m. The return air roadway 4106 suffers from the mining of the working face 4105 and will suffer from the secondary mining of the working face 4106 in the future. The relative position of the roadway is shown in Figure 1.

The surrounding rock of the strong mining roadway with a large coal pillar in the BinHuang mining area is characterized by severe deformation, long-term creep and asymmetric deformation and failure. The deformation of the roadway in the advance section of the working face is large, the phenomenon of roadway spalling is serious, the roof subsidence appears as mesh pockets and floor heaving, and the bolt and anchor cable lock fall off. The deformation and failure of the return air roadway 4106 mainly manifest as roof subsidence, uneven bulge and floor heaving. It has seriously affected the smooth progress of the working face and safe and efficient production. The deformation and failure characteristics of a similar roadway and return air roadway 4103 as shown in Figure 2.

3. Analysis of Deformation Characteristics of Strong Mining Roadway

3.1. FLAC3D Numerical Model Establishment

3.1.1. FLAC^{3D} Numerical Model and Boundary Conditions. The length × width × height of the model are 268 m × 100 m × 79 m. The upper boundary load is calculated based on the mining depth of 700 m. The top of the model is a free surface with a vertical load of 15.25 MPa, and a 1.8 lateral pressure coefficient, the mining height is 9.5 m, the coal pillar width is 44.5 m, the bottom boundary of the model is fixed in the vertical direction, and the left and right boundaries are fixed in the horizontal direction.

The roof is supported by eight bolts with a diameter of 22 mm and a length of 2500 mm in each row. The prestress of each bolt is 30 kN and the row spacing is 800 mm. In addition, each row has five anchor cables with a diameter of 21.8 mm and a length of 7100 mm. The prestress of each anchor cable is 130 kN, and the row spacing is 800 mm. On the two sides of the roadway there is a row of five anchors for support with a diameter of 22 mm and a length of 2500 mm. The prestress of each bolt is 30 kN and the row spacing is 800 mm.

The model adopts the Mohr–Coulomb yield criterion, the numerical calculation model is shown in Figure 3, and the rock layer occurrence and mechanical parameters are shown in Table 1.

3.2. Deformation and Failure Law of Roadway Surrounding Rock during the First Mining

3.2.1. Displacement Distribution Law. The roadway displacement distribution after the mining of working face 4105 is shown in Figure 4.

As shown in Figure 4, the total roof subsidence after the mining of adjacent working face 4105 is 615 mm, the total floor deformation is 545 mm, the total deformation of the mining sidewall is 774 mm, and the total deformation of the

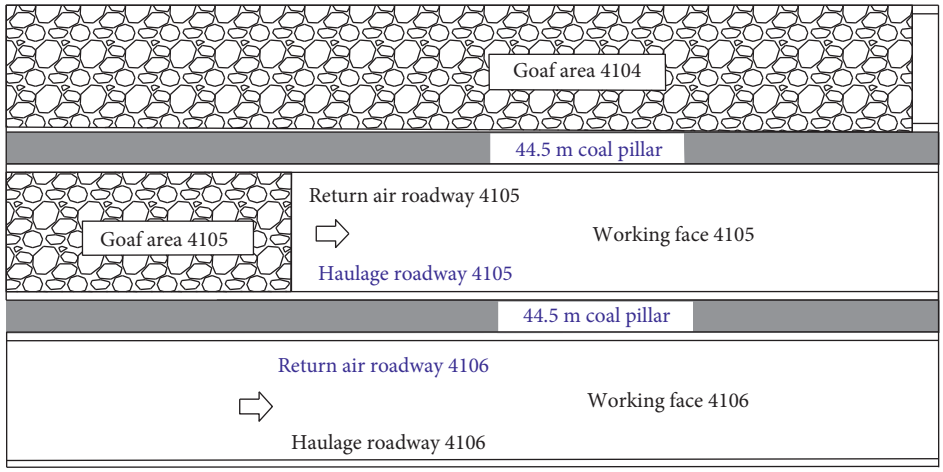

Figure 1: Relative position of return air roadway 4106.

(a) (b)

Figure 2: Deformation and failure characteristics of similar roadway, i.e., return air roadway 4103. (a) Roof sinking. (b) Floor heaving.

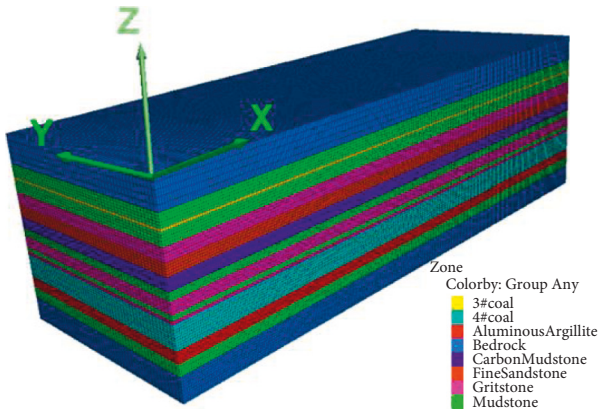

Figure 3: Numerical calculation model.

pillar sidewall is 662 mm. It can be seen that the roadway deformation is dominated by two sides during the first mining.

3.2.2. Stress Distribution Law. The 3D stress nephogram and vertical stress distribution of the 3-meter layer above the roadway roof after the mining of working face 4105 are shown in Figures 5 and 6, respectively.

From Figures 5 and 6, it can be seen that after the mining of working face 4105, the key blocks formed by the breaking of the main roof of the goaf are rotated and sunk under the action of rotary torque, and the lateral abutment pressure is formed near the goaf side of the coal pillar. The peak abutment pressure is 28.3 MPa, the stress concentration coefficient is 1.63, and the peak stress point is 25 m from the coal wall of the goaf in working face 4105 and 19.5 m from the pillar sidewall of the roadway.

3.3. Deformation and Failure Law of Roadway Surrounding Rock during the Secondary Mining

3.3.1. Displacement Distribution Law. In order to further clarify the deformation and failure characteristics of roadways at different distances in a working face advance under secondary mining, the slice cloud images of vertical and horizontal displacements at 0, 10, 20, 40, 60 and 80 m in the working face advance are obtained. The deformation characteristics of the roadway at different distances in the working face advance are shown in Figure 7.

The statistics of roadway deformation at different positions away from the working face are summarized in Table 2 during the first and the secondary mining stages.

Table 1: Rock layer distribution and mechanical parameters.

Lithology	Thickness (m)	Density ($kg \cdot m^{-3}$)	Bulk modulus (GPa)	Shear modulus (GPa)	Internal friction angle (°)	Tensile strength (MPa)	Cohesion (MPa)
Mudstone	38.4	2589	5.87	3.97	32	4.09	1.1
#3 coal	1.1	1386	2.12	1.8	29	0.5	0.8
Mudstone	5.1	2589	5.87	3.97	32	4.09	1.1
Coarse sandstone	5.3	2264	2.42	2.15	38	2.48	1.8
Fine sandstone	4.8	2395	2.10	1.76	36	3.17	1.7
Carbonaceous mudstone	5.1	2314	2.22	1.81	28	1.5	0.8
Mudstone	3.3	2589	5.87	3.97	32	4.09	1.1
Coarse sandstone	4.8	2264	2.42	2.15	38	2.48	1.8
Mudstone	2	2489	3.87	1.97	32	2.09	1.0
Coarse sandstone	1.4	2264	2.42	2.15	38	2.48	1.8
#4 coal	9.5	1324	1.97	1.5	27	0.4	0.6
Aluminum mudstone	4.6	2314	2.22	1.81	28	0.5	0.8
Mudstone	14.6	2489	3.87	1.97	32	2.09	1.0

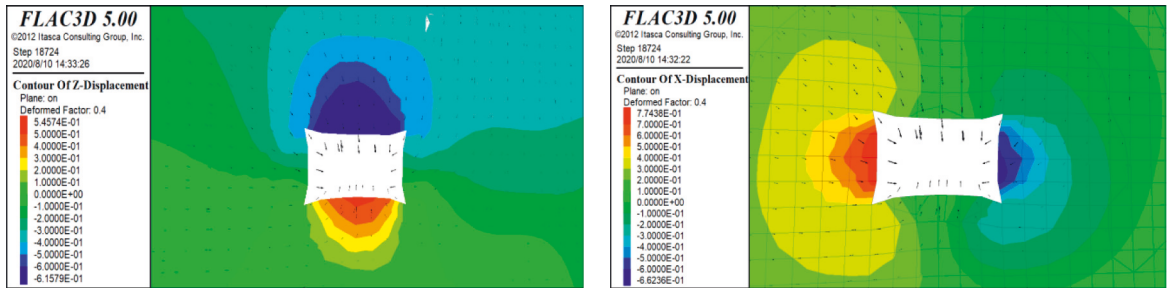

(a) (b)

Figure 4: Roadway deformation law of first mining. (a) First mining—vertical displacement distribution. (b) First mining—horizontal displacement distribution.

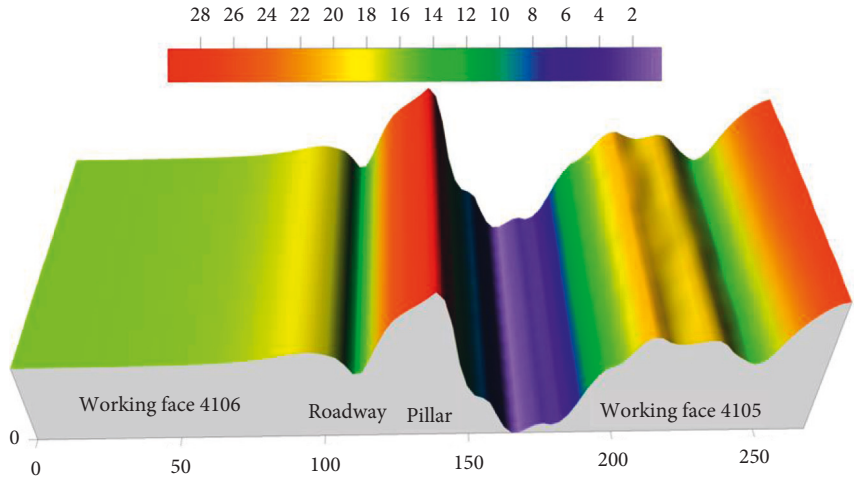

Figure 5: Three-dimensional stress distribution of surrounding rock after the mining of working face 4105.

It can be seen from Table 2 that the total deformation of the roof and floor is 1160 mm, and the total shrinkage deformation of the two sides is 1436 mm; the deformation of roadway is dominated by the shrinkage of the two sides during the first mining. The total deformation of the roof and floor of the roadway in the working face advance gradually increased from 1737 mm 80 m away from the working face to 2281 mm at the working face, and the total deformation of the two sides gradually increased from 2094 mm 80 m away from the working face to 2211 mm at the working face; the deformation of the mining sidewall was greater than that of the pillar sidewall during the secondary mining.

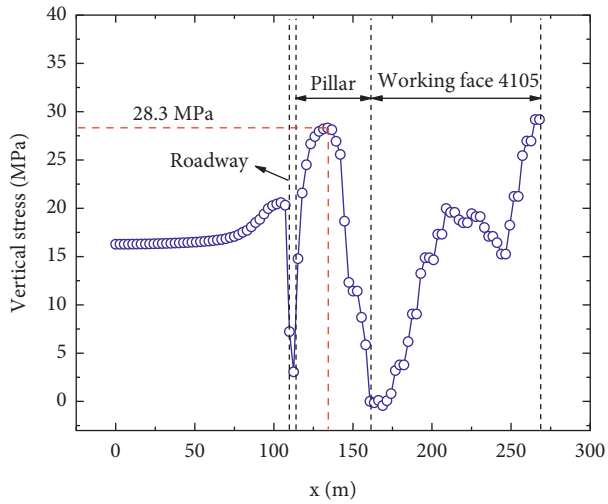

Figure 6: Vertical stress distribution of roof during the mining of working face 4105.

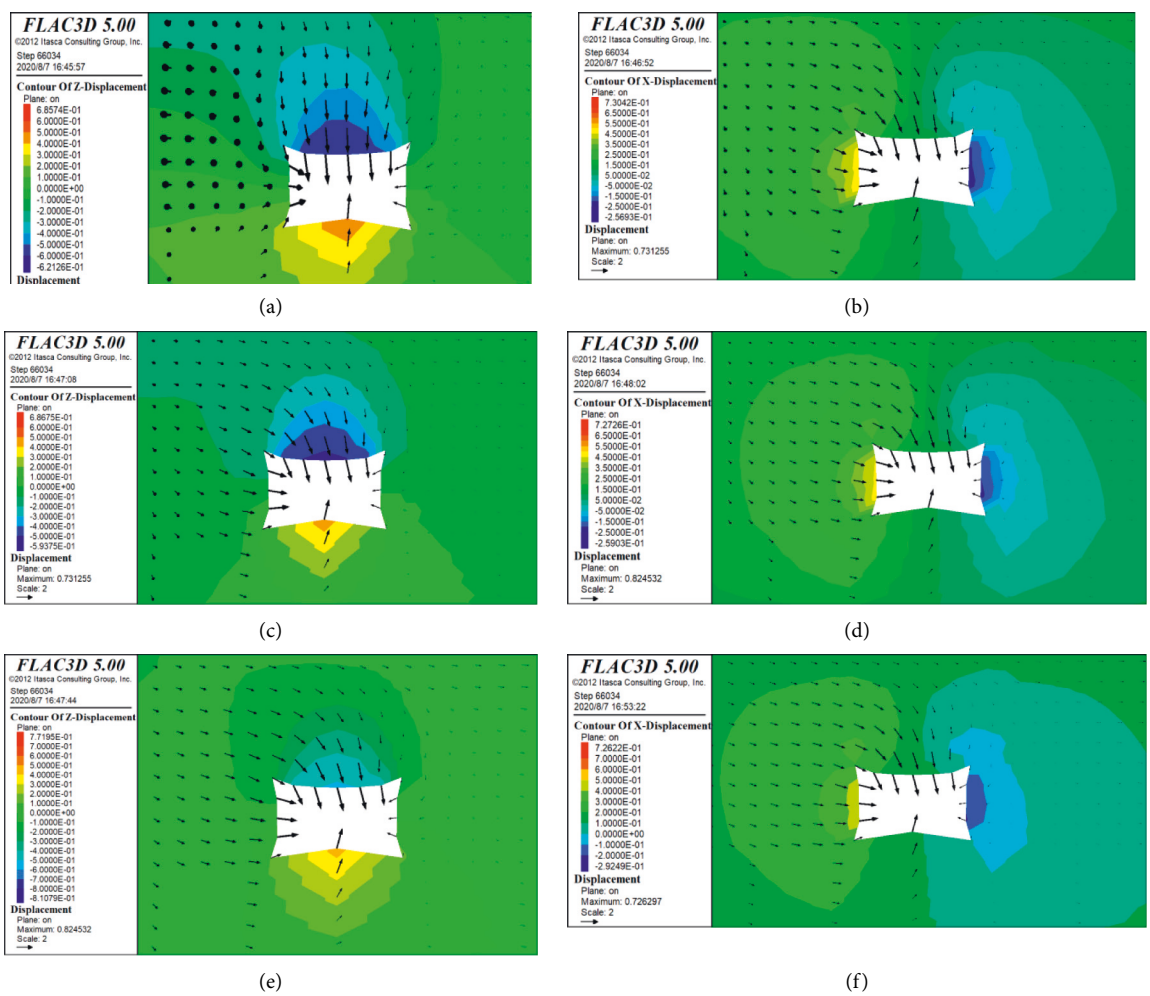

Figure 7: Continued.

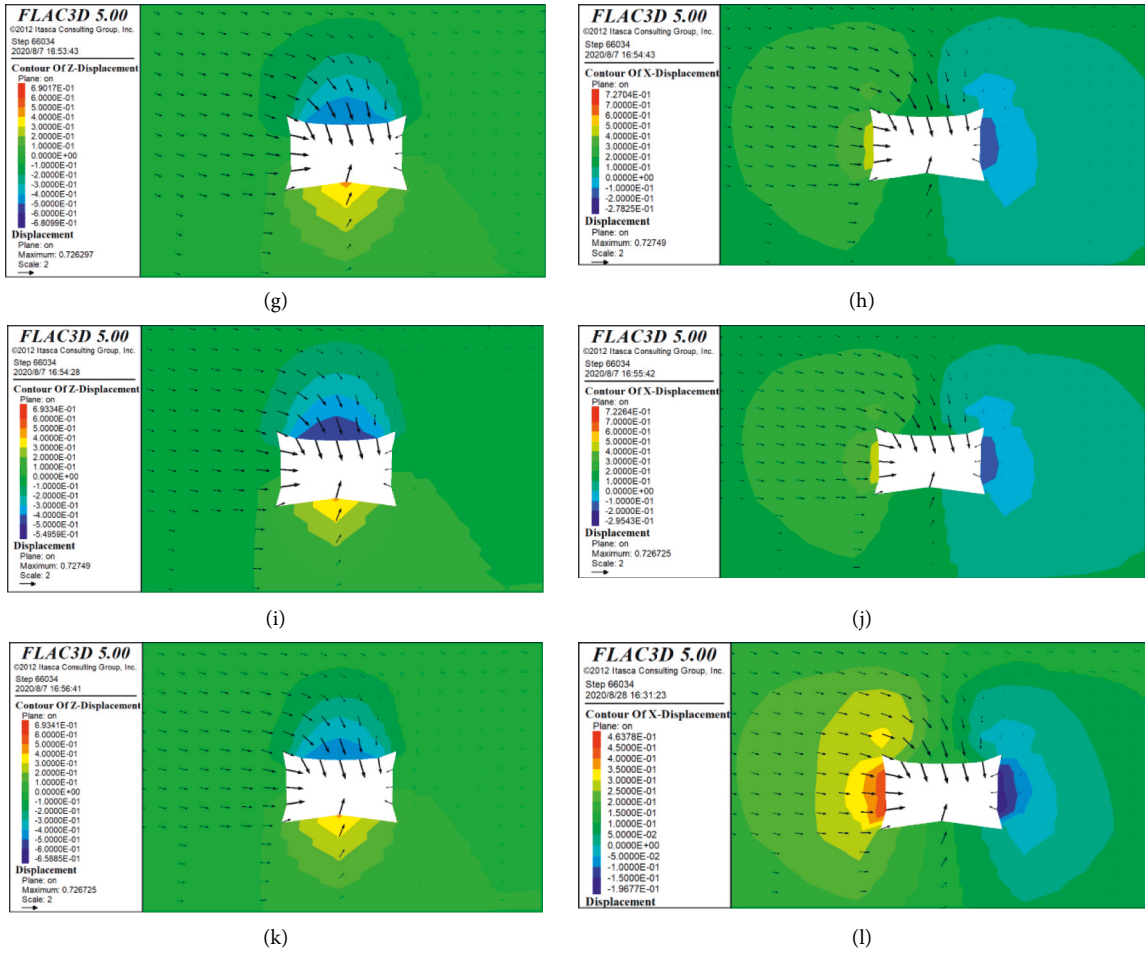

Figure 7: Deformation characteristics of roadway in working face advance. (a) Vertical displacement of 0 m in advance of working face. (b) Horizontal displacement of 0 m in advance of working face. (c) Vertical displacement of 10 m in working face advance. (d) Horizontal displacement of 10 m in working face advance. (e) Vertical displacement of 20 m in working face advance. (f) Horizontal displacement of 20 m in working face advance. (g) Vertical displacement of 40 m in working face advance. (h) Horizontal displacement of 40 m in working face advance. (i) Vertical displacement of 60 m in working face advance. (j) Horizontal displacement of 60 m in working face advance. (k) Vertical displacement of 80 m in working face advance. (l) Horizontal displacement of 80 m in working face advance.

Table 2: Deformation and failure characteristics of roadway under different engineering disturbances (unit: mm).

	First mining	Secondary mining (leading head-on distance)					
		0 m	10 m	20 m	40 m	60 m	80 m
Roof	615	1236	1208	1065	1065	1065	1065
Floor	545	1045	1008	993	976	965	962
Mining sidewall	774	1276	1257	1250	1239	1236	1236
Pillar sidewall	662	954	898	883	870	860	858

3.3.2. Stress Distribution Law. The three-dimensional stress nephogram after secondary mining and the vertical stress distribution law of rock mass in the advance of the working face after first mining and secondary mining are shown in Figures 8(a) and 8(b).

It can be seen from Figures 8(a) and 8(b) that the key block formed by the breaking of the main roof of the goaf under the action of rotary moment causes rotary subsidence, and the lateral abutment pressure is formed near the side of the coal pillar to the goaf side. The peak abutment pressure is 28.3 MPa, the stress concentration coefficient is 1.61, and the peak stress point is 19.5 m away from the coal pillar of the roadway. After secondary mining, the peak value of lateral abutment pressure of the coal pillar is 36.7 MPa, the stress concentration coefficient is 2.1, the peak point offsets 10 m to the side of the roadway, and the peak position is 9.5 m away from the roadway coal wall. The vertical stress peak near the coal wall aggravates the deformation of the roadway after secondary mining and increases the difficulty of maintaining the secondary mining roadway.

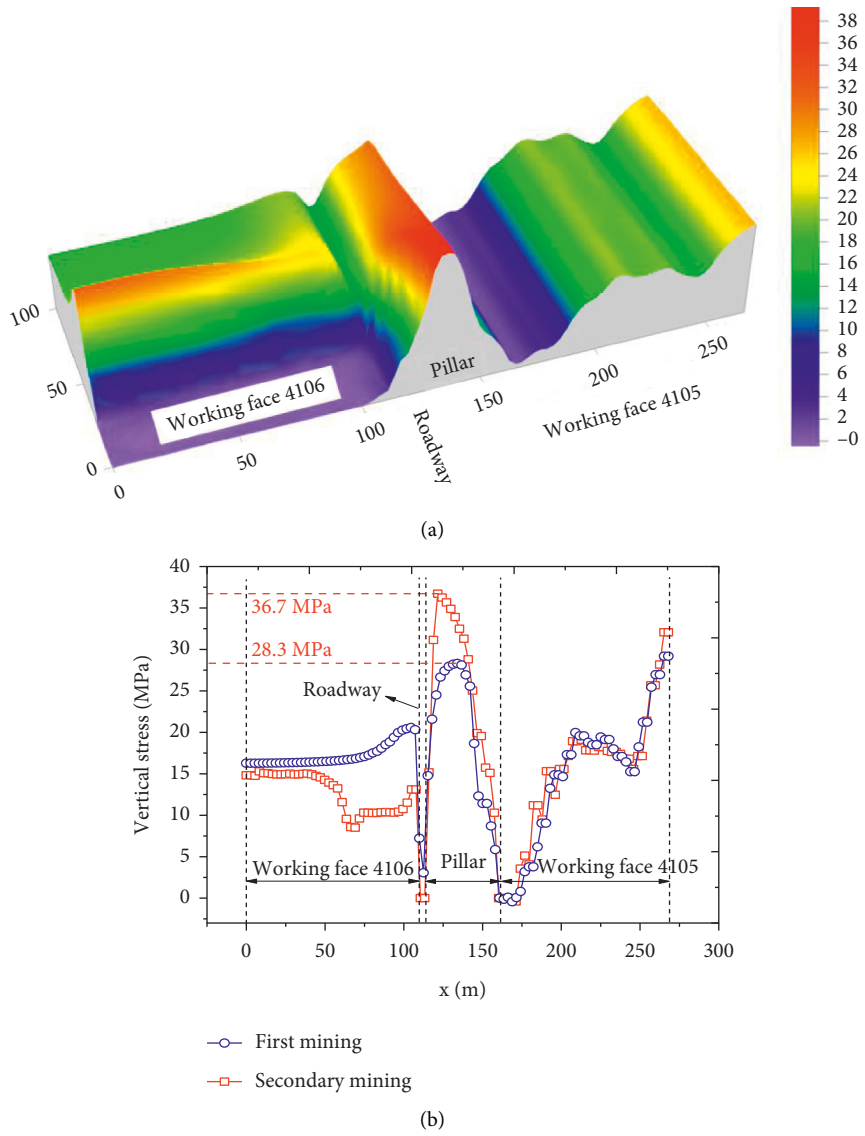

FIGURE 8: Three-dimensional stress nephogram of secondary mining and vertical stress distribution of roadway surrounding rock. (a) Three-dimensional stress nephogram. (b) Distribution law of vertical stress in surrounding rock of roadway.

The distribution law of abutment pressure in the advance of excavating and mining the working face is shown in Figure 9.

It can be seen from Figure 9 that after roadway excavation, the maximum vertical stress of working face 4106 is 18.8 MPa, and the stress concentration coefficient is 1.07. After the mining of working face 4105, the lateral abutment pressure increases the maximum vertical stress of working face 4106 to 23.8 MPa, and the stress concentration coefficient is 1.34. With the mining of working face 4106, the main roof strata in the goaf are gradually broken and become unstable. The cantilever beam structure of the goaf causes the stress concentration in the advance of the working face. The maximum vertical stress is 32.5 MPa, the stress concentration coefficient is 1.85, and the maximum stress concentration position is 18.6 m in the advance of the working face.

For the roadways experiencing secondary mining, the damage caused by the advanced abutment pressure and the lateral abutment pressure of the coal pillar in the secondary mining is far more than that caused by the roadway driving period and the first mining period. Overall, it presents sudden instability, which significantly increases the deformation of the roof and floor of the roadway and the two sides, and makes maintaining the secondary mining roadway more difficult.

4. Control Countermeasures and Engineering Practice

4.1. Long Anchorage and Stress Relief Collaborative Control Technology. The pretightening force of the normal bolt is low, and the anchorage length is insufficient. When the deformation occurs outside the anchorage zone and exceeds the support range of the bolt, the roof may be separated, and support failure occurs. Therefore, the roof should adopt long anchorage technology, and the continuous beam of the thick

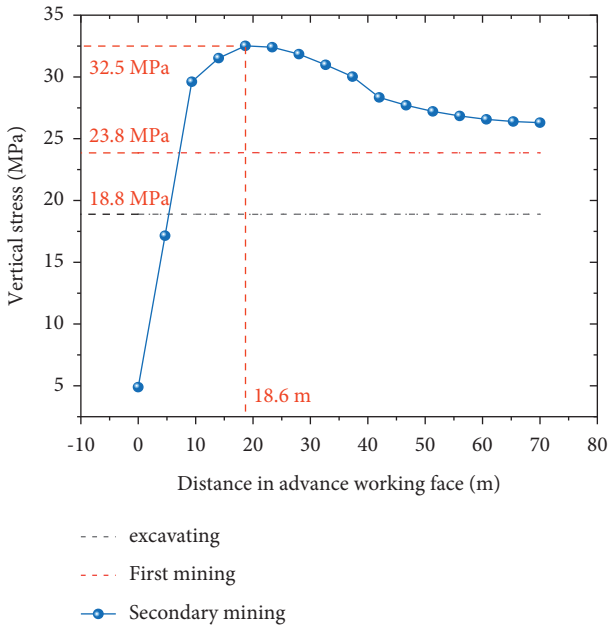

Figure 9: Distribution law of abutment pressure in advance.

anchorage layer should be constructed using a long anchor bolt. The anchorage rock beam is formed as a whole, and the bending stiffness of the thick anchorage beam is increased. The roof is transformed from the load body to the bearing body, and the roof subsidence decreases. The bearing body transmits the load of the overlying strata to the deep part of the two sides of the coal body, thereby reducing the load of the shallow coal body of the two sides and transferring the load of the roof to the floor, which effectively controls the roadway.

The stress relief of cutting and blasting the roof concentrates charge blasting at the bottom of the surrounding rock drilling, which destroys the rock stratum. After blasting, many artificial fractures appear, which separates the surrounding rock near the roadway from the deep rock mass. The rock strata, originally in a high stress state, are unloaded, and the stress is transferred to the deep surrounding rock. Stress relief blasting can not only release the elastic deformation energy accumulated in the rock mass, but also, under the action of stress relief blasting, the loose circle itself is compressed and compacted. At a certain time, the loose circle produced by stress relief blasting can directly absorb the deformation of the surrounding rock, thereby reducing the deformation of the surrounding rock.

4.2. Roadway Support Schemes. According to the numerical simulation analysis, although the stress relief under the original scheme can better optimize the stress of the surrounding rock, multiple mining operations caused the roadway surrounding rock to be seriously deformed. Combined with the field investigation, the bolt length in the original support is too short, and the bolt is in the roof fracture development zone. Under the influence of strong mining, the thickness of the roof anchorage layer of the roadway is small, and the shallow and deep anchorage layers cannot play a linkage role, which cannot achieve the maintenance effect of coordinated bearing. The anchorage system has weak resistance to mining and cannot reasonably control the strong mine pressure problem of the roadway with large deformation under strong mining.

In view of these problems existing in roadway maintenance under the support of the original scheme, the new scheme adopts a new thick-layer high-strength bearing ring surrounding rock strengthening technology to deal with the influence of strong mining. Compared with the original scheme, the new scheme increases the length of the roof bolt. At the same time, two anchor cables are added to the pillar sidewall to solve the easy deviation of the pillar sidewall problem. The thick anchor layer is constructed by the bolt (cable), and the "stress relief-anchoring" integrated control of the surrounding rock of the roadway is realized.

Specific supporting parameters of the roadway: the roof of the roadway is supported by prestressed flexible long bolt and steel mesh, it is arranged in rows of eight bolts, and the whole bolts and steel mesh are vertical to the roof. The anchorage force is no less than 120 kN. The top net adopts Φ6.0-millimeter steel mesh with specifications of 5600×1000 mm. A row of high prestressed anchor cables, five in each row, is arranged in the middle of each row of anchors in the roof, and the anchor cables are fully perpendicular to the roof. The spacing is 1200 mm, and the row spacing is 1600 mm (during the advance mining of working face 4105, the final row spacing of the roof anchor cables is 800 mm). The anchoring force is no less than 200 kN. The supports of the two sides of the roadway are combined and are supported by five ultra-high-strength prestressed bolts made of grade IV left spiral steel and eight wire meshes. The bolt torque is not less than 200 N m. The mesh was made of eight wire meshes 40×40 mm in size with a specification of 4200×1100 mm. The support parameters of return air roadway 4106 are shown in Figure 10.

4.3. Design of Stress Relief Scheme for Roadways. The roof of return air roadway 4106 was subjected to deep hole blasting with roof cutting upward in the pillar sidewall. The opening position was 1.5 m away from the pillar sidewall, and the final hole was in the coal pillar of haulage roadway 4105. The length of the stress relief borehole was 34 m in the east-west direction and 28 m in the vertical direction. The stress relief schematic diagram of return air roadway 4106 is shown in Figure 11. The construction parameters of roadway drilling are shown in Table 3.

4.4. Analysis of Roadway Support Effect. The roadway surface displacement reflects the deformation of the roadway surface and the degree of reduction in the roadway section including the roof, the floor and the two sides; it has a reference value to judge whether the movement of the surrounding rock exceeds its safely allowable value and whether it affects the normal use of the roadway. In order to master the surrounding rock activity characteristics and the stability law of return air roadway 4106 during the first mining period and verify the control effect of the high-efficiency flexible long

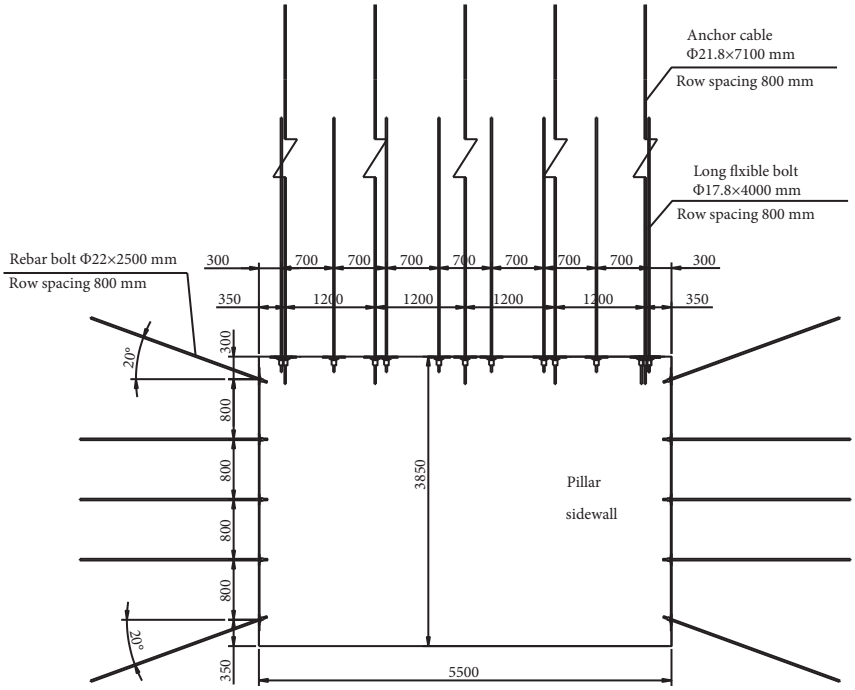

Figure 10: Support parameters of the return air roadway 4106.

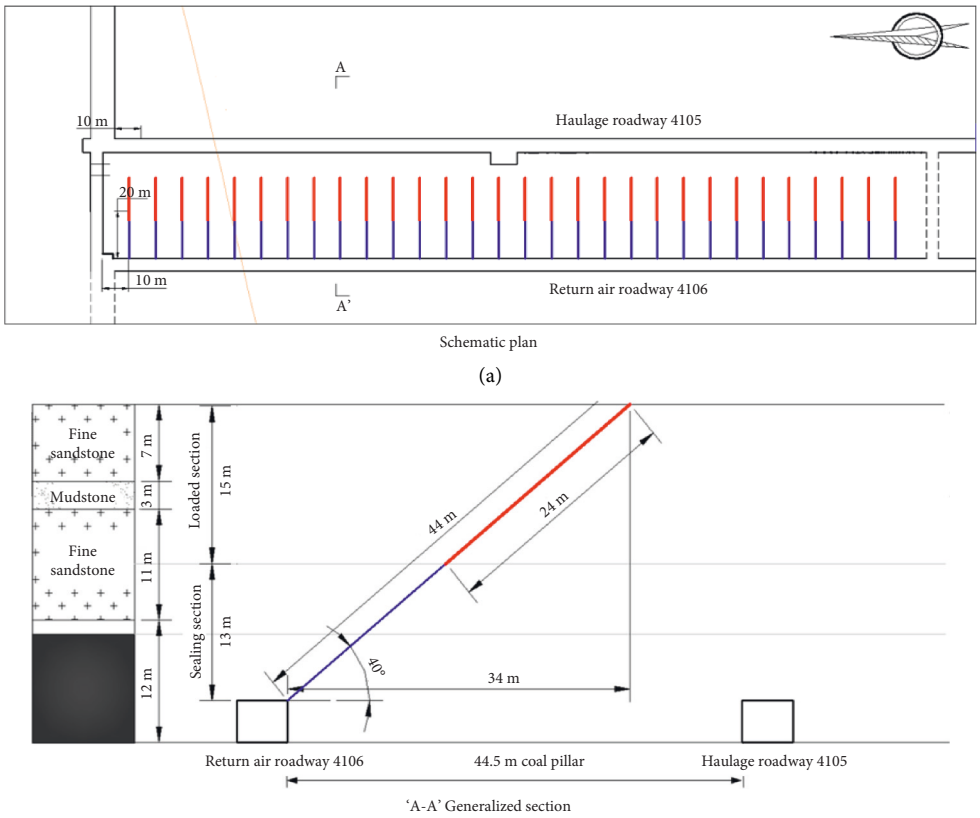

Figure 11: Schematic diagrams of stress relief scheme in return air roadway 4106. (a) Schematic plan. (b) "A-A" generalized section.

Table 3: Drilling construction parameters of return air roadway 4106.

Construction location	Drilling type	Borehole inclinometer (°)	Drilling angle (°)	Drilling diameter (mm)	Drilling depth (m)
The top angle of the mining sidewall of return air roadway 4106	Presplitting blasting in roof	90	40	75	44
Borehole spacing (m)	Loaded length (m)	Loaded length (section)	Loading amount (kg)	Hole sealing length (m)	
10	24	60	66	20	

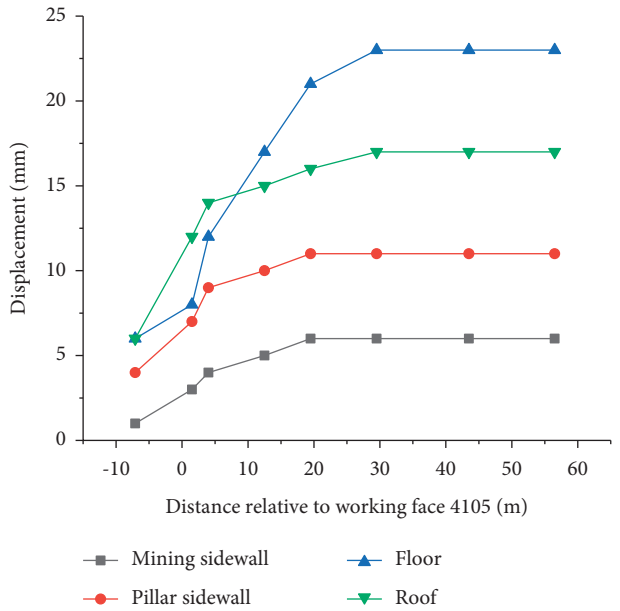

Figure 12: Displacements of the return air roadway 4106 versus distance to working face 4105.

Figure 13: Photos of Roadway maintenance effect.

anchor and roof cutting blasting stress relief technology on the roadway, the station was arranged to cover 2812.75 m of the roadway to monitor the surface displacement of the surrounding rock during the mining of the working face. The surface displacement of return air roadway 4106 versus the distance to the working face is shown in Figure 12.

It can be seen from Figure 12 that in the 0–20-meter section away from the working face, the roadway is strongly affected by mining. After 30–40 m away from the fully mechanized caving face, the deformation area of the roadway is stable. Overall, the deformation of the roof and the floor of the roadway is greater than that of the two sides. The maximum deformation of the roof is 17 mm, the maximum deformation of the pillar sidewall is 11 mm, the maximum deformation of the mining sidewall is 6 mm, and the maximum deformation of floor heaving is 23 mm. The deformation of the roadway is far lower than that of the original support scheme. The separation values of the deep and shallow roof are both 1 mm. The high-efficiency long anchorage and roof cutting blasting stress relief have a good effect on the control of the roadway. The specific maintenance effects are shown in Figure 13.

5. Conclusions

(1) During the first mining, the total deformation of the roof and the floor was 1160 mm, and the total shrinkage deformation of the two sides was 1436 mm; the deformation of the roadway was dominated by the shrinkage of the two sides. During the second mining, the total deformation of the roof and floor of the roadway in the working face advance gradually increased from 1737 mm 80 m away from the working face to 2281 mm at the working face, and the total deformation of the two sides gradually increased from 2094 mm 80 m away from the working face to 2211 mm at the working face. The deformation of the mining sidewall was greater than that of the pillar sidewall. After first mining, the peak abutment pressure of coal pillar was 28.3 MPa, the stress concentration coefficient was 1.61, and the stress peak point was 19.5 m from the pillar sidewall of the roadway.

(2) After secondary mining, the peak value of lateral abutment pressure of coal pillar was 36.7 MPa, the stress concentration coefficient was 2.1, and the peak point was shifted to the roadway side by 10 m. The peak value of vertical stress near the coal wall aggravated the deformation of the roadway after secondary mining. For the roadway experiencing secondary mining, the stress concentration factor caused by the superposition of the lateral abutment pressure of the coal pillar and the head-on advanced abutment pressure of the secondary mining was much larger than that during the roadway's first mining period. Overall, the roadway presented sudden instability caused by the abnormal stress concentration, which made the deformation of the roof and floor of the roadway and the two sides increase, and maintenance of the secondary mining roadway more difficult.

(3) Based on field investigation, theoretical analysis and the results of numerical simulation, the collaborative control technology of long anchorage-top-cutting blasting stress relief was proposed, and an industrial test was carried out. The engineering application shows that the mining influence distance during the first mining was about 30~40 m, the maximum roof subsidence was 17 mm, the maximum deformation of pillar sidewall was 11 mm, the maximum deformation of mining sidewall was 6 mm, and the maximum floor heaving was 23 mm. The support effect is excellent.

Data Availability

The data used to support the findings of the study are included in the article.

Conflicts of Interest

The authors declare that they have no conflicts of interest.

Acknowledgments

This work was financially supported by the Fundamental Research Funds for the Central Universities (Grant no. 2018QNA27) and the National Natural Science Foundation of China (Grant no. 51704277).

References

[1] H. P. Kang and P. F. Jiang, B. X. Huang, G. Xuemao, W. Zhigen et al., Roadway strata control technology by means of bolting-modification-destressing in synergy in 1 000 m deep coal mines," *Journal of China Coal Society*, vol. 45, no. 3, pp. 845–864, 2020.

[2] S. Q. Yang, M. Chen, H. W. Jing, K. F. Chen, and B. Meng, "A case study on large deformation failure mechanism of deep soft rock roadway in Xin'An coal mine, China," *Engineering Geology*, vol. 217, pp. 89–101, 2017.

[3] H. Wang, S. Xue, Y. Jiang, D. Deng, S. Shi, and D. Zhang, "Field investigation of a roof fall accident and large roadway deformation under geologically complex conditions in an underground coal mine," *Rock Mechanics and Rock Engineering*, vol. 51, no. 6, pp. 1863–1883, 2018.

[4] X. W. Feng, N. Zhang, F. Xue, Z. Z. Xie, Practices, experience, and lessons learned based on field observations of support failures in some Chinese coal mines," *International Journal of Rock Mechanics and Mining Sciences*, vol. 123, Article ID 104097, 2019.

[5] L. Sun, H. Wu, and B. Yang, Q. Li, Support failure of a high-stress soft-rock roadway in deep coal mine and the equalized yielding support technology: a case study," *International Journal of Coal Science & Technology*, vol. 2, no. 4, pp. 279–286, 2015.

[6] X. X. Chen, L. C. Wang, D. H. Fu, A study on inward movement deformation mechanism and control technology of dynamic pressure gateway of island mining face," *Journal of Mining & Safety Engineering*, vol. 32, no. 4, pp. 552–558, 2015.

[7] W. J. Wang, C. Yuan, W. J. Yu et al., "Control technology of reserved surrounding rock deformation in deep roadway under high stress," *Journal of China Coal Society*, vol. 41, no. 9, pp. 2156–2164, 2016.

[8] H. Yan, F. L. He, L. Y. Li, R. Feng, and P. Xing, "Control mechanism of a cable truss system for stability of roadways within thick coal seams," *Journal of Central South University*, vol. 24, no. 5, pp. 1098–1110, 2017.

[9] F. X. Xie, F. L. He, S. F. Yin, J. K. Wu, and G. C. Zhang, "Study on asymmetric control of large section gob-side coal entry influenced by strong mining," *Journal of Mining & Safety Engineering*, vol. 33, no. 6, pp. 999–1007, 2016.

[10] S. Fang and J. Zhang, "In-situ measure to internal stress of shotcrete layer in soft-rock roadway," *International Journal of Coal Science & Technology*, vol. 1, no. 3, pp. 321–328, 2014.

[11] G. C. Zhang and F. L. He, "Asymmetric failure and control measures of large cross-section entry roof with strong mining disturbance and fully-mechanized caving mining," *Chinese Journal of Rock Mechanics and Engineering*, vol. 35, no. 4, pp. 806–818, 2016.

[12] C. W. Luo, H. B. Li, and Y. Q. Liu, "Characteristics of in-situ stress and variation law of plastic zone surrounding rocks around deep tunnels in a coal mine," *Chinese Journal of Rock Mechanics and Engineering*, vol. 30, no. 8, pp. 1613–1618, 2011.

[13] B. J. Du, C. Y. Liu, F. F. Wu, and J. X. Yang, "Deformation mechanism and control technology of roadway in deep mine with high stress and weak surrounding rock," *Journal of Mining & Safety Engineering*, vol. 37, no. 6, pp. 1123–1132, 2020.

[14] M. Wang, X. Y. Wang, and T. Q. Xiao, "Borehole destressing mechanism and determination method of its key parameters in deep roadway," *Journal of China Coal Society*, vol. 42, no. 5, pp. 1138–1145, 2017.

[15] H. P. Kang, "Seventy years development and prospects of strata control technologies for coal mine roadways in," *China" Chinese Journal of Rock Mechanics and Engineering*, vol. 40, no. 1, pp. 1–30, 2020.

[16] Y. Ma, H. W. Jing, and Y. H. Chen, "Numerical simulation of failure mechanism of surrounding rocks in mining induced roadway and its support," *Journal of Mining & Safety Engineering*, vol. 24, no. 1, pp. 109–113, 2007.

[17] Y. W. Lan, Y. J. Zhang, and H. M. Gao, "Research on the mechanism of floor heaving of roadway in deep mining," *Mining Research and Development*, vol. 25, no. 1, pp. 34–36, 2005.

[18] H. P. Kang and J. H. Wang, *Coal Roadway Roof Bolt Support Theory and Complete Set of Technology*, Coal Industry Press, Beijing, 2007.

[19] B. X. Huang, N. Zhang, and H. W. Jing, "Large deformation theory of rheology and structural instability of the surrounding rock in deep mining roadway," *Journal of China Coal Society*, vol. 45, no. 3, pp. 911–926, 2020.

[20] N. Zhang, X. H. Li, and M. S. Gao, "Pretensioned support of roadway driven along next gob and heading adjacent advancing coal face and its application," *Chinese Journal of Rock Mechanics and Engineering*, vol. 23, no. 12, pp. 2100–2105, 2004.

[21] X. H. Li, H. M. Yang, H. X. Liu, and F. Q. Wang, "Research on bolt-grouting reinforcement technology in dynamic pressure and soft rock roadway," *Journal of Mining & Safety Engineering*, vol. 23, no. 2, pp. 159–163, 2006.

[22] S. B. Yang, M. C. He, W. T. Liu, and X. J. Ma, "Mechanics and application research on the floor anchor to control the floor heaving of deep soft rock roadway," *Chinese Journal of Rock Mechanics and Engineering*, vol. 27, pp. 2913–2920, 2008.

[23] H. B. Zhao, H. Cheng, J. Y. Li, T. Wang, Y. H. Liu, and F. Y. Qin, "Study on asymmetric deformation mechanism of surrounding rock of roadway under the effect of isolated coal pillar," *Chinese Journal of Rock Mechanics and Engineering*, vol. 39, no. S1, pp. 2771–2784, 2016.

[24] Q. Wang, P. Zhang, and Z. H. Jiang, "Automatic roadway formation method by roof cutting with high strength bolt-grouting in deep coal mine and its validation," *Journal of China Coal Society*, vol. 46, no. 2, pp. 382–397, 2021.